engineering proceedings

Proceeding Paper

Local Area Improvement of GSM Network Coverage †

Miroslav Tomov [1], Panagiotis Kogias [2], Michail Malamatoudis [2] and Stanimir Sadinov [1,*]

1 Department of Communications Equipment and Technologies, Technical University of Gabrovo, 5300 Gabrovo, Bulgaria; mtomov@tugab.bg
2 Department of Physics, International Hellenic University, St. Lucas, 65404 Kavala, Greece; kogias@teiemt.gr (P.K.); malamatoudismichail@yahoo.gr (M.M.)
* Correspondence: murry@tugab.bg

† Presented at the 4th International Conference on Communications, Information, Electronic and Energy Systems (CIEES 2023), Plovdiv, Bulgaria, 23–25 November 2023.

Abstract: This article describes the design of a local GSM signal amplifying system and presents the results of appliance performance measurements, simulations and analyses. The system consists of a receiving antenna of the Yagi type, a 50 Ω cable, a 0.5–1.5 GHz wideband RF amplifier and a transmitting antenna. A precise measurement of the S-parameters of each component is performed and recorded in the appropriate S-matrix data file format. The amplifying system is first realized in a Keysight Genesys programming simulation platform with S-models, created based on the measured data. That schematic is simulated and optimized by calculating additional impedance-matching circuits included in the initial schematic design.

Keywords: GSM signal; amplifying; S-parameters

check for updates

Citation: Tomov, M.; Kogias, P.; Malamatoudis, M.; Sadinov, S. Local Area Improvement of GSM Network Coverage. *Eng. Proc.* **2024**, *60*, 24. https://doi.org/10.3390/engproc2024060024

Academic Editor: Renato Filjar

Published: 17 January 2024

1. Introduction

Despite the requirements and the "promises" of the providers, the quality of mobile telecommunication services is not adequate in some parts of their covered areas. In fact, the radio signal coverage of the GSM network, and the level of the LTE signal in particular, is not reliable, nor is it constantly stable enough in the areas of small villages where few people live, although the majority of those people also need a mobile service with the same excellent parameters as is delivered in the territories of the big cities [1,2]. Obviously, it is not profitable for the providers to develop the infrastructure in low-population areas, and this is a very unpleasant problem for the minority population who prefer to live in small towns and villages or much closer to wild nature [3].

The present paper displays some interesting results and analyses of the design and exploration of a local radio signal amplifying system, developed to receive, amplify, transmit and spread GSM signals across a small area of a village home yard [4].

NanoVNA-FV2 has been used for the measurements concerning the components of the GSM [5] signal local amplifying system—parameters of the antennas, cables and RF amplifier. For the measurements of parameters of the radio signal coverage both the RF Field Strength Analyzer Protek 3200 and the mobile Android OS application Network Cell Info has been used [6].

2. Schematic Design of the Amplifying System

2.1. Initial Schematic Design

The initial schematic of the designed GSM signal amplifying system is shown in Figure 1. The receiving antenna type is a nine-element Yagi with the appropriate dimensions of its elements for optimal performance in the range of frequencies of 850 to 950 MHz, with vertical polarization; it is pointed towards the closest base station of the GSM network.

The location of the antenna is on the roof of the house, and the direction has been established after some pre-calculations based on the GPS data concerning the latitude and longitude of the nearest 4G-supporting base station of the GSM service provider. The position and direction of the antenna were precised by RF signal measurement. The antenna is equipped with an RG-58 50 Ω coax cable with an N-type female connector [7].

The receiving antenna is equipped with an RG-58 50 Ω coax feeder cable and an N-type female connector. A convertor, N-type male to SMA female, couples the antenna feeder to the RG-58 coax cable. Both outputs of the cable are equipped with SMA male connectors—the first one is connected to the SMA female side of the convertor, N to SMA, and the second one is connected to the input terminal of the RF power amplifier [8].

The second coax cable links the output of the amplifier and the distribution antenna connector (also N-type female). That cable is also equipped with SMA male connectors at both of its ends, which necessitates one more convertor, SMA male to N-type male.

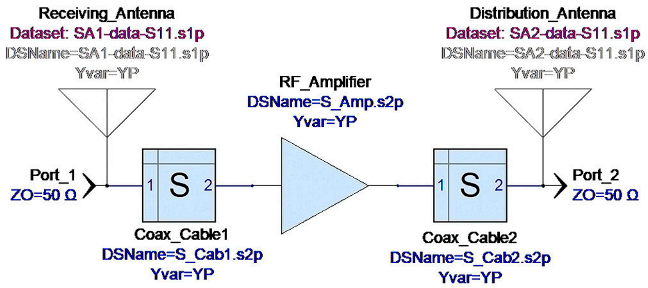

Figure 1. Block schematic of the designed GSM signal amplifying system.

Although it appears to be more convenient to terminate the respective outputs of the coax cables directly with the appropriate connectors (N-type male) and to avoid the need for convertors, there is an important reason for the described arrangement. The described schematic is designed for the initial measurement and simulation without the need for impedance-matching components in the network.

2.2. Final Schematic Topology and Components of the Local GSM Signal Amplifying System

As soon as the simulation provided the results, it has been evident that the impedance sequence had to be ensured between the receiving antenna and amplifier, and between the amplifier and the load, i.e., the distribution antenna. The impedance-matching schematic units to be inset in the input network and in the load network were designed with discrete elements based on the results of the simulation. These units also needed the respective optimization concerning the connector arrangements, but this could be done only after their best possible place in the topology had been established during the process of simulation.

3. Consecution of Measurements and Results

3.1. Measurement of S-Parameters of the Amplifying System Components by NanoVNA-FV2

The main purpose of the measurement has been to collect the S-parameters data matrix of each of the components of the amplifying system in order to prepare an accurate simulation model to ensure the maximal coincidence between the real and expected electromagnetic behavior of the amplifying system.

The S-parameters measurement has been performed individually for each component of the initial schematic on Figure 1 [9].

Both the receiving antenna and the distribution antenna are one-port devices, so the following parameters were measured and recorded [10] in an .s1p file format by the vector network analyzer: S11 Smith chart, |S11|, return loss, characteristic impedance, R + jX, input signal phase, group delay of the input signal, quality factor, serial C, serial L, real/imaginary, R/omega, X/omega.

The RF power amplifier as well as both linking coax cables are two-port devices (quadrupoles), so the measured parameters by the same instrument are S11 (S22), S21 (S12), S11 Smith chart, |S11|, return loss, characteristic impedance, R + jX, input signal phase, group delay of the input signal, quality factor, serial C, serial L, real/imaginary, R/omega, X/omega, S21 polar plot, gain, |S21|, output signal phase, group delay of the output signal, S11 and S21 comparison (LogMag) and time domain response (TDR).

One of the remarkable and important functionalities of the vector network analyzer NanoVNA-FV2 is the calibration procedure available before each measurement. In the case of two-port devices, the calibration applies a set of three special connectors terminating the measuring circuit to open and short and to a 50 Ω load. Once the calibration is done, it can be saved in a file for later use when the same measurement schematic arrangements are applied.

In the case of two-port devices being tested, an additional calibration procedure is performed, called "through". It connects PORT1 to PORT2 directly by a benchmark coaxial single cable or by a pair cable, connected by a standard SMA adaptor, as is depicted in Figure 2. The calibration of the analyzer effectively eliminates the greatest majority of undesired impedances across the measuring network caused by the self-reactance of all connectors, convertors, etc. that impact the accuracy of the measurement of such high-frequency radio signals (close to 1 GHz). After the calibrating procedure of the instrument, the measurements are performed.

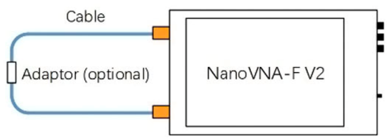

Figure 2. Schematic of the vector analyzer calibration procedure "through".

3.2. Measured Data Results and Graphics

3.2.1. Receiving Antenna Equipped with RG-58 50 Ω Coax Feeder Cable, N-Type Female Connector

A convertor, N-type male to SMA female, couples the antenna feeder to the calibrated coax cable of the instrument.

The Smith chart of the receiving antenna is shown in Figure 3, and the voltage standing wave ratio (VSWR) as a function of the frequency in the GSM signal band is depicted in Figure 4. In the Smith chart, it is evident that the impedance of the antenna does not match the 50 Ω load across the entire GSM band. The closest point to the center of the chart is in the very beginning of the frequency range explored, i.e., 850 MHz. The worst value of the VSWR is 2.885, reached at 944.6 MHz—corresponding to the most outlying point relative to the center of the Smith chart.

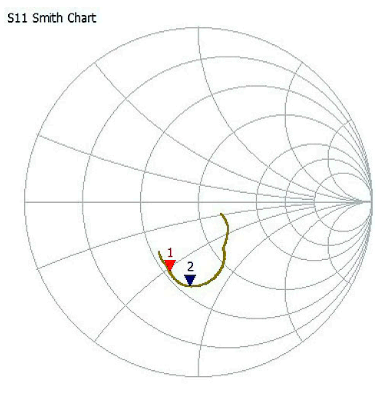

Figure 3. Smith chart of the receiving antenna.

The analysis of the measurements led to the conclusion that an impedance-matching component has to be added to the input network of the amplifying system, between the receiving antenna and the RF amplifier input port (Figure 5). The exact parameters and place of the matching circuit were determined after the simulation.

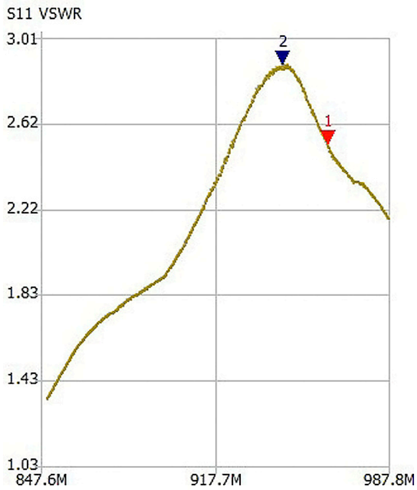

Figure 4. VSWR of receiving antenna across the GSM signal frequency band.

Marker 1

Frequency:	963.082 MHz	VSWR:	2.518
Impedance:	26.94 -j26.5 Ω	Return loss:	-7.300 dB
Admittance:	52.96 -j53.9 Ω	Quality factor:	0.983
Series L:	-4.3753 nH	S11 Phase:	-112.07°
Series C:	6.2417 pF	S21 Gain:	-62.289 dB
Parallel R:	52.96 Ω	S21 Phase:	52.19°
Parallel X:	3.0669 pF		

Marker 2

Frequency:	944.906 MHz	VSWR:	2.885
Impedance:	28.78 -j36.4 Ω	Return loss:	-6.281 dB
Admittance:	74.74 -j59.1 Ω	Quality factor:	1.263
Series L:	-6.1257 nH	S11 Phase:	-95.48°
Series C:	4.6314 pF	S21 Gain:	-62.585 dB
Parallel R:	74.735 Ω	S21 Phase:	82.96°
Parallel X:	2.8476 pF		

Figure 5. Measured parameters of the receiving antenna at marked frequencies.

3.2.2. Distribution Antenna Also Equipped with RG-58 50 Ω Coax Feeder Cable, N-Type Female Connector

An N-type male to SMA female convertor couples the antenna feeder to the calibrated coax cable of the instrument.

The Smith chart of the distribution antenna is shown in Figure 6, and the voltage standing wave ratio (VSWR) as a function of the frequency in the GSM signal band in Figure 7. On the Smith chart, it is evident that the impedance of the distribution antenna, which is practically the load of the amplifying system, is close to the ideal 50 Ω load across the entire GSM band.

The closest point to the center of the chart is near the end of the frequency range explored, i.e., 961.8 MHz. The best value of the VSWR is 1.009 (Figure 7) and it is reached at the same frequency—961.8 MHz, which corresponds to the most outlying point from the center of the Smith chart.

The distribution antenna obviously achieves much better values of the same parameters, compared to the receiving antenna.

The distribution antenna obviously achieved better values for the Smith chart and VSWR parameters, compared to the receiving antenna. But the receiving antenna shows a bigger value of the gain (Figure 8) for the chosen frequencies from the same range. The gain of the receiving antenna is around −62 dB and the gain of the distribution antenna is about −87 dB.

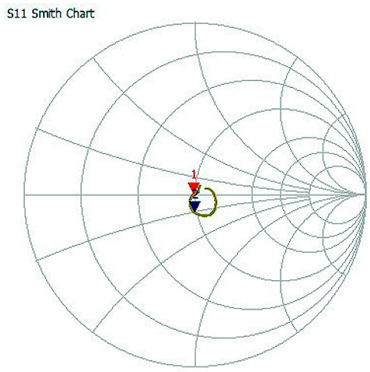

Figure 6. Smith chart of the distribution antenna.

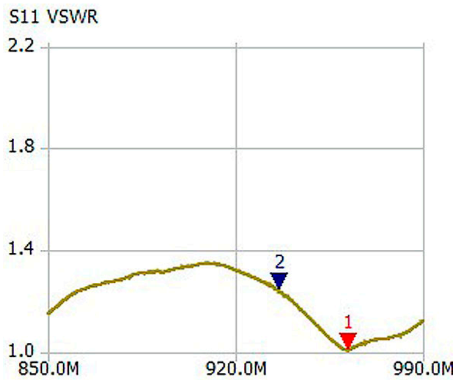

Figure 7. VSWR of distribution antenna across the GSM band.

On all diagrams, the blue marker shows the frequency of the biggest gain, and the red marker shows the frequency of the best impedance match, i.e., the best power efficiency across the band.

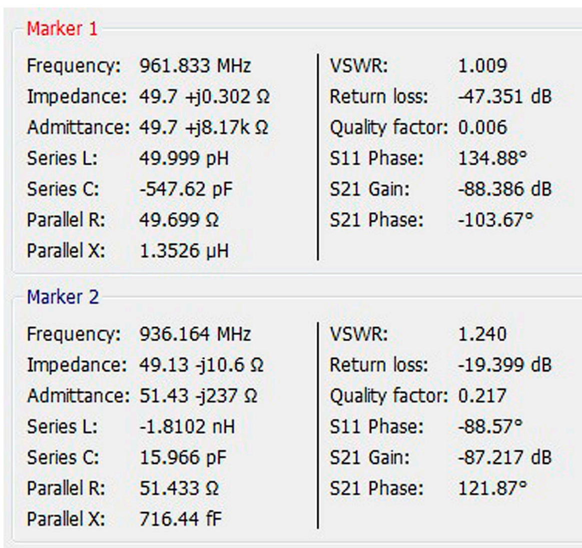

Marker 1

Frequency:	961.833 MHz	VSWR:	1.009
Impedance:	49.7 +j0.302 Ω	Return loss:	-47.351 dB
Admittance:	49.7 +j8.17k Ω	Quality factor:	0.006
Series L:	49.999 pH	S11 Phase:	134.88°
Series C:	-547.62 pF	S21 Gain:	-88.386 dB
Parallel R:	49.699 Ω	S21 Phase:	-103.67°
Parallel X:	1.3526 μH		

Marker 2

Frequency:	936.164 MHz	VSWR:	1.240
Impedance:	49.13 -j10.6 Ω	Return loss:	-19.399 dB
Admittance:	51.43 -j237 Ω	Quality factor:	0.217
Series L:	-1.8102 nH	S11 Phase:	-88.57°
Series C:	15.966 pF	S21 Gain:	-87.217 dB
Parallel R:	51.433 Ω	S21 Phase:	121.87°
Parallel X:	716.44 fF		

Figure 8. Measured parameters of the distribution antenna at marked frequencies.

The appropriate parameters, topology and place of the impedance-matching circuit were determined after the simulation.

The design of the local GSM amplifying system has been developed through the optimization of the S-matrix of the system in the simulation environment.

4. Simulation and Analysis for Optimization

The S-parameters model of the real RF amplifier was used in the simulation schematic. Similarly, S-matrix models were prepared to present correctly the behavior of the connecting coax cables. The parameters of those models depend on the length of each particular cable [11].

The impedance-matching schematics (Figure 9) at the input and load network of the amplifying system were designed with discrete passive elements, whose parameters were calculated automatically by the programming module, part of the simulation program and based on Matlab.

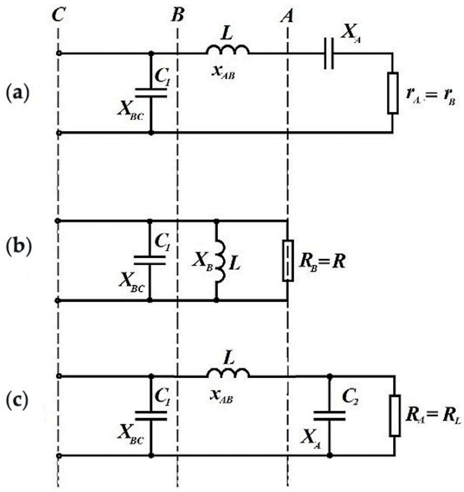

Figure 9. Equivalent circuit for impedance conversion from parallel to series topology (**a**); equivalent circuit for impedance conversion from series to parallel topology (**b**); Impedance-matching circuit without any conversion (**c**).

X_A, X_B are the reactances after the respective dotted line; X_{AB}, X_{BC} are the reactances between the respective dotted lines; C_1, C_2, L represents the capacitances and inductance of the respective lumped elements in the circuits; R_A, r_A r_B represents the respective resistances in the circuits, R_L is the load.

Impedance-matching components (Figure 9) were calculated by applying the following mathematical model [9,12]:

$$r_A = R_B = \frac{R_A}{1+q_A^2} = \frac{R_L}{1+q_A^2}, \tag{1}$$

$$x_A = \frac{X_A}{1+\frac{1}{q_A^2}}, \tag{2}$$

The load quality factor is

$$Q_L = \frac{X_{AB}}{r_A}, \tag{3}$$

The series reactance to the right of line b is

$$x_A = x_{AB} - x_A = (Q_L - q_A)r_A, \tag{4}$$

The quality factor of the reactance to the right of line b is

$$q_B = \frac{x_B}{r_B} = \frac{R}{X_B} = \frac{R}{X_{BC}}, \tag{5}$$

The active and reactive components of the matched impedance Z are obtained by (4):

$$R_B = R = r_B\left(1 + q_B^2\right) \quad (6)$$

and

$$X_B = x_B\left(1 + \frac{1}{q_B^2}\right) \quad (7)$$

The values of the above-mentioned physical quantities were calculated automatically in the simulation environment, which provided an integrated Matlab programming module, and Equations (1)–(7) above were preset in advance.

5. Conclusions

The results and analysis of the measurements show that it is necessary to inset an impedance-matching component also in the output network of the amplifying system, between the RF amplifier output port and the distribution antenna. Assuming the fixed construction of the antennas, the components that can be improved are the RF amplifier, the length of the cable to optimal values and the parameters of the discrete elements of the impedance-matching transformation circuits.

The exploration of the problem could be expanded towards the goals of reaching more effective RF power distribution of the GSM signal at a particular place, concerning the achievement of higher data traffic speed in areas of weak network coverage, supplied by the GSM service provider. The main quality parameters of the RF signal in the GSM network discussed in this exploration are the maximum and average power values of the distributed signal and real data traffic speed.

The present paper displays some practical results and analyses of the design and exploration of a local RF amplifying system, developed to receive, amplify, transmit and spread LTE and 4G GSM signals across a small area of a village home yard where 4G service signal is very weak or not reliable.

Author Contributions: Conceptualization, M.T. and S.S.; methodology, M.T.; software, M.T.; validation, P.K., M.M. and S.S.; formal analysis, P.K.; investigation, M.T.; resources, S.S.; data curation, P.K.; writing—original draft preparation, M.T.; writing—review and editing, S.S.; visualization, M.M.; supervision, P.K.; project administration, M.M.; funding acquisition, M.M. All authors have read and agreed to the published version of the manuscript.

Funding: This research received no external funding.

Institutional Review Board Statement: Not applicable.

Informed Consent Statement: Not applicable.

Data Availability Statement: The data can be obtained from the corresponding author upon request.

Acknowledgments: The presented work is supported under project 2205E/2023 "Planning, design and optimization of wireless communication platforms, services and solutions for 5G and IoT applications" by the University Centre for Research and Technology at the Technical University of Gabrovo. Thanks to all staff of the Department of Communications Equipment and Technologies at the Technical University of Gabrovo and of the Department of Physics at the International Hellenic University in Kavala.

Conflicts of Interest: The authors declare no conflicts of interest.

References

1. Iliev, I. *Mobile Communications*; TU-Sofia: Sofia, Bulgaria, 2014.
2. Mihaylov, G.Y.; Iliev, T.B.; Bikov, T.D.; Ivanova, E.P.; Stoyanov, I.S.; Keseev, V.P.; Dinov, A.R. Test cases and challenges for mobile network evolution from LTE to 5G. In Proceedings of the 41st International Convention on Information and Communication Technology, Electronics and Microelectronics, Opatija, Croatia, 21–25 May 2018; pp. 449–452. [CrossRef]

3. Iliev, T.B.; Mihaylov, G.Y.; Bikov, T.D.; Ivanova, E.P.; Stoyanov, I.S.; Radev, D.I. LTE eNB traffic analysis and key techniques towards 5G mobile networks. In Proceedings of the 2017 40th International Convention on Information and Communication Technology, Electronics and Microelectronics (MIPRO), Opatija, Croatia, 22–26 May 2017; pp. 497–500. [CrossRef]
4. Blaunstein, N.; Christodoulou, C.G. *Radio Propagation and Adaptive Antennas for Wireless Communication Networks*, 2nd ed.; Wiley: Hoboken, NJ, USA, 2014.
5. Hamam, R.; Karalis, A.; Joannopoulos, J.; Soljacic, M. Coupled-mode theory for general free-space resonant scattering of waves. *Phys. Rev. A* **2007**, *75*, 53801. [CrossRef]
6. Raab, F.H.; Asbeck, P.; Cripps, S.; Kenington, P.B.; Popovich, Z.B.; Pethecary, N.; Sevic, J.F.; Sokal, N.O. RF and Microwave Power Amplifier and Transmitter Technologies—Part 2. *High Freq. Electron.* **2003**, *2*, 39–48.
7. Grebennikov, A. *RF and Microwave Power Amplifier Design*; McGraw-Hill: New York, NY, USA, 2004; p. 433.
8. Nedelchev, I.; Tomov, M. Optimization of High Efficient RF Power Amplifying Schematics by Automated S-matrix Analysis. In *Proceedings of the Scientific Conference of Angel Kanchev University of Rousse, Rousse, Bulgaria, 28–29 October 2016*; Series 3.2; Angel Kanchev University of Rousse: Rousse, Bulgaria, 2016; Volume 55, pp. 8–12.
9. Kazimierczuk, M. *RF Power Amplifiers*; TK7871.58.P6K39; John Wiley & Sons: Hoboken, NJ, USA, 2008.
10. Nedelchev, I.; Tomov, M. Optimized Gain Achievement At Efficiency Over 90% And Minimized Noise of RF Power Amplifiers by S-parametric Correction. In Proceedings of the UNITECH'2016—Gabrovo, Gabrovo, Bulgaria, 18–19 November 2016; Volume II, pp. 168–172.
11. Nedelchev, I.; Sadinov, S.; Tomov, M. Radio Frequency Parallel Circuit Class E Power Amplifier. In Proceedings of the UNITECH'2016—Gabrovo, Gabrovo, Bulgaria, 18–19 November 2016; Volume II, pp. 102–107.
12. Weber, R.J. *Introduction to Microwave Circuits: Radio Frequency and Design Applications*; IEEE Press Series on RF and Microwave Technology; John Wiley & Sons: Hoboken, NJ, USA, 2001; Volume xvi, 431p.